

Marinoquinolines A–F, Pyrroloquinolines from *Ohtaekwangia kribbensis* (Bacteroidetes)

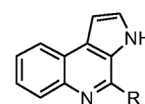
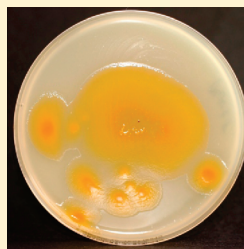
Patrick W. Okanya,^{†,‡} Kathrin I. Mohr,[†] Klaus Gerth,[†] Rolf Jansen,[†] and Rolf Müller^{*,†,‡}

[†]Helmholtz Centre for Infection Research, Work Group Microbial Drugs, Inhoffenstrasse 7, 38124 Braunschweig, Germany

[‡]Helmholtz Institute for Pharmaceutical Research and Department of Pharmaceutical Biotechnology, Saarland University, P.O. Box 15115, 66041 Saarbrücken, Germany

S Supporting Information

ABSTRACT: Marinoquinoline A (**1**) was isolated from the gliding bacterium *Ohtaekwangia kribbensis* together with the novel marinoquinolines B–F (**2**–**6**). Their structures were elucidated from NMR and HRESIMS data. The pyrroloquinolines showed weak antibacterial and antifungal activities and moderate cytotoxicity against four growing mammalian cell lines with IC_{50} values ranging from 0.3 to 8.0 $\mu\text{g}/\text{mL}$. In a screening against tropical parasites marinoquinolines A–F (**1**–**6**) showed activity against *Plasmodium falciparum* K1 with IC_{50} values between 1.7 and 15 μM .



Marinoquinoline A R = methyl

Marinoquinoline B–F
R = alkyl, aryl or heteroaryl

In our continued screening for novel secondary metabolites from gliding bacteria, marinoquinoline A (**1**) and the five marinoquinoline derivatives **2**–**6** were isolated from strain PWU 25. Marinoquinoline A (**1**) has previously been isolated from the novel marine bacterium *Rapidithrix thailandica*¹ and characterized by X-ray crystallography² as an inhibitor of acetylcholine esterase.³ Our producing strain PWU 25 showed 99.9% similarity after 16S rDNA classification to the recently described bacterium *Ohtaekwangia kribbensis*.⁴ Herein, we report the isolation of marinoquinolines A–F (**1**–**6**), their MS- and NMR-based structure elucidation, and their biological activities.

All marinoquinolines were isolated from a 70 L batch fermentation of *O. kribbensis*, strain PWU 25, performed in the presence of Amberlite XAD 16 adsorber resin. The products were extracted from the resin and separated by acid–base solvent partitioning, Sephadex LH-20 chromatography, and RP-HPLC.

Ultra-high-resolution ESIMS (UHRESIMS) and isotopic pattern analysis of the pseudomolecular ion at m/z 183.0919 $[M + H]^+$ revealed the molecular formula $C_{12}H_{10}N_2$ for the main product **1**, which allowed identification of two possible structures, i.e., marinoquinoline A (**1**) and the pyridoindole isomer harman (**7**).⁵ Since **1** had been characterized previously solely by X-ray analysis, the structural details were elucidated from a series of 1D and 2D NMR experiments in acetone- d_6 (Table 1). The ^{13}C NMR spectrum showed signals for all carbon atoms, and all carbon-bound proton signals were correlated with their corresponding carbon signals from an $^1\text{H},^{13}\text{C}$ HMQC NMR spectrum.

The remaining NH proton was detected as a broad singlet at $\delta_{\text{H}} = 11.12$ ppm, while the methyl group C-10 appeared as a singlet at $\delta_{\text{H}} = 2.83$ ppm, typical of aromatic methyl groups. The

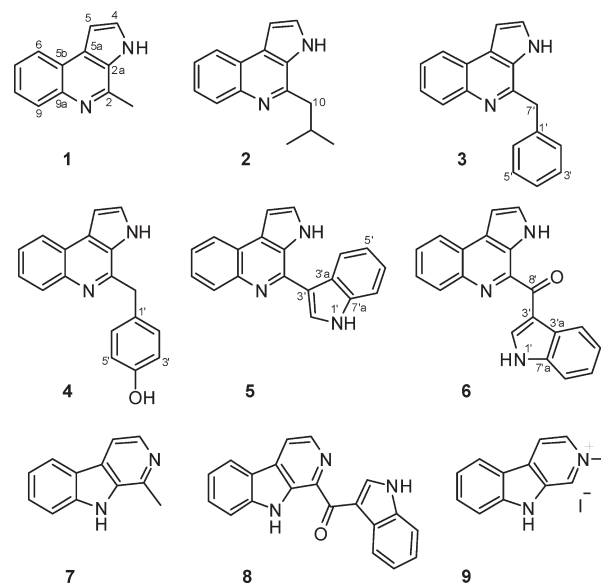


Figure 1. Marinoquinolines A–F (**1**–**6**) and structural analogues **7**–**9**.

$^1\text{H},^1\text{H}$ COSY NMR spectrum indicated the presence of a pair of aromatic protons (H-4 and H-5) and of four aromatic protons (H-6 to H-9) in an *ortho*-disubstituted ring, which was completed by the quaternary carbons C-9a and C-5b (Figure 2).

Carbon C-9a was identified from strong $^1\text{H},^{13}\text{C}$ HMBC correlations with H-6 and H-8, while C-5b was assigned from

Received: September 4, 2010

Published: April 01, 2011



HMBC correlations with H-6, -7, and -9. Similarly, the HMBC correlations of the quaternary carbon atoms C-5a and C-2a each with H-4 and H-5 allowed the assignment of the pyrrole ring. The assignment was supported by the small vicinal coupling of 2.8 Hz between H-4 and H-5 and by the observation of the direct $^1\text{H}, ^{13}\text{C}$ coupling constants $^1J_{\text{H,C}} = 173$ and 184 Hz for methines H-5 and H-4, respectively, which are characteristic of pyrrole systems similar to the one found in **1**.⁵

The HMBC correlation of C-5a with H-6 and the only NOE of **1** between H-5 and H-6 indicated the connection of the aromatic rings. A further correlation of C-2a with H-10 and the single HMBC correlation of C-2 with the methyl protons H-10 were consistent with the position of the methyl group at C-2. In particular, the absence of any further correlations of the methyl group bearing C-2 is compatible only with the isomer marinoquinoline A (**1**). Finally, we were able to recrystallize **1** and to replicate the X-ray structure according to Kanjana-opas et al.²

HRESIMS analysis of marinoquinoline B (**2**) revealed a $[\text{M} + \text{H}]^+$ ion at m/z 225.1382, consistent with the molecular formula $\text{C}_{15}\text{H}_{16}\text{N}_2$. As with all marinoquinolines studied in this investigation, the $^1\text{H}, ^1\text{H}$ COSY and $^1\text{H}, ^{13}\text{C}$ HMQC and HMBC correlations indicated the pyrroloquinoline core structure. Two new methyl group signals 12-H₃ and 13-H₃, overlapping as an aliphatic doublet at $\delta_{\text{H}} = 1.00$ ppm, and a multiplet of a methine H-11 at $\delta_{\text{H}} = 2.44$ ppm were observed in the ^1H spectrum of **2**. They belong to an isopropyl side chain that replaces the methyl group at C-2 of marinoquinoline A (**1**) in **2** according to their COSY correlations and to HMBC correlations between C-10 and H-12, H-13, and H-11. The connection of the side chain was confirmed by the HMBC correlation of C-2 with H-10 and H-11.

The molecular formula $\text{C}_{18}\text{H}_{14}\text{N}_2$ was indicated from the $[\text{M} + \text{H}]^+$ ion at m/z 259.1236 in the HRESIMS analysis of marinoquinoline C (**3**). Besides the pyrroloquinoline core structure in **3** (Table 2) all further carbon-bound proton signals in the novel phenyl ring in **3** were correlated with their corresponding carbon signals from a $^1\text{H}, ^{13}\text{C}$ HMQC NMR spectrum. The

additional phenyl ring was assigned from the $^1\text{H}, ^1\text{H}$ COSY correlations of the aromatic protons and from the HMBC correlations observed, for example, between C-6' and H-4' and H-2' or between C-1' and H-5' and H-3'.

Curiously, no HMBC correlations were observed with the methylene group C-7' initially, though this remained as the only perfect link to complete structure **3**. However, during NMR measurements the protons at C-7' were exchanged against deuterium from the acetone- d_6 solvent and their singlet signal, in the beginning observed in a ^1H NMR spectrum, was no longer present during later NMR experiments. The unexpected H/D exchange can be explained by keto–enol tautomerism of acetone- d_6 providing deuterium ions. The enolization was catalyzed by the basic alkaloid **3** itself, and it was verified by HRESIMS of the deuterated molecular ion at m/z 261.1351, calcd for 261.1361 $[\text{C}_{18}\text{H}_{12}\text{N}_2\text{D}_2 + \text{H}]^+$. The H/D exchange at the methylene group bridging both aromatic systems was reversible.

HRESIMS analysis of marinoquinoline D (**4**) revealed a $[\text{M} + \text{H}]^+$ ion at m/z 275.1181 with the molecular formula $\text{C}_{18}\text{H}_{14}\text{N}_2\text{O}$, indicating an additional oxygen atom compared to **3**. Unlike **3**, marinoquinoline D (**4**) was only poorly soluble in acetone. Hence its NMR data were collected in methanol- d_4 (Table 2). All carbon-bound proton signals in the new *p*-phenol unit were correlated with their corresponding carbon signals from a $^1\text{H}, ^{13}\text{C}$ HMQC NMR spectrum. The phenol carbon atom

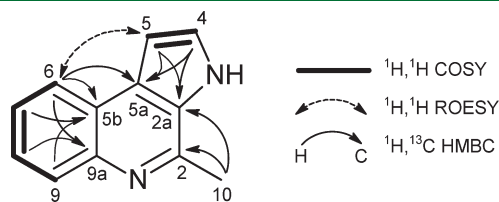


Figure 2. Selected 2D NMR correlations of marinoquinoline A (**1**).

Table 1. NMR Spectroscopic Data of Marinoquinolines A (**1**) and B (**2**) in Acetone- d_6

C/H	1 ^a			2 ^b		
	δ_{H} , m (J in Hz)	δ_{C} ^c	HMBC ($^1J_{\text{C,H}}$ in Hz)	δ_{H} , m (J in Hz)	δ_{C} ^c	HMBC ($^1J_{\text{C,H}}$ in Hz)
2		146.92, qC	10		149.99, qC	10
2a		129.89, qC	4, 5, 10		129.69, qC	4, 5, 10,
NH	11.12, br s			11.16, br s		
4	7.57, d (2.8)	127.11, CH	5 (184 Hz)	7.57, d (2.9)	127.05, CH	5 (184 Hz)
5	7.12, d (2.8)	102.04, CH	4 (173 Hz)	7.12, d (2.9)	101.87, CH	4 (174 Hz)
5a		128.41, qC	4, 5, 6		128.64, qC	4, 6 > 5
5b		124.26, qC	7, 9 > 6		124.01, qC	7, 9
6	8.22, dd (7.7, 2.0)	123.77, CH	8 > 7	8.23, d (7.7, 1.8)	123.66, CH	8
7	7.48, td (7–8, 2.0) ^d	125.71, CH	9 (163 Hz)	7.51, td (7–8, 2.0) ^d	125.63, CH	9
8	7.51, td (7–8, 2.0) ^d	126.11, CH	6 (163 Hz)	7.51, td (7–8, 2.0) ^d	126.05, CH	6
9	7.99, dd (7.7, 2.0)	129.98, CH	7, 6	8.04, d (7.7, 1.8)	129.87, CH	7
9a		143.89, qC	6, 8 > 9		143.53, qC	6, 7/8
10	2.83, s	21.34, CH ₃	(120 Hz)	3.08, d (7.3)	43.91, CH ₂	12/13, >11
11				2.44, tspt (7.3, 6.8)	29.01, CH	10, 12/13
12				1.00, d (6.8)	22.96, CH ₃	10, 13 > 11
13				1.00, d (6.8)	22.96, CH ₃	10, 12 > 11

^a $^1\text{H}/^{13}\text{C}$ 600/150 MHz. ^b $^1\text{H}/^{13}\text{C}$ 600/75 MHz. ^c ^{13}C data are given with two digits in order to discriminate between narrowly separated signals.

^d Second-order multiplets.

Table 2. NMR Spectroscopic Data of Marinoquinolines C (3) and D (4)

C/H	3 ^a			4 ^b		
	δ_{H} , m (J [Hz])	δ_{C} ^c	HMBC	δ_{H} , m (J [Hz])	δ_{C} ^c	HMBC
2		148.98, qC	n.o. ^d		148.83, qC	7'
2a		129.20, qC	5		128.76, qC ^e	4, 5
NH	11.15, br s			8.44, br s		
4	7.55, d (2.9)	127.47, CH	5	7.85, d (2.8)	133.21, CH	5
5	7.12, d (2.9)	102.10, CH	4	7.30, d (3.0)	103.42, CH	4
5a		129.39, CH	4 > 5, 6		132.87, qC	5, 6
5b		124.30, qC	7		124.77, C	9, 7/8
6	8.24, d (6.2)	123.83, CH	8	8.12, d (1.0)	124.77, CH	7/8
7	7.51, td (7.3, 2.2)	126.06, CH	9	7.71, m	127.77, CH	9
8	7.54, td (8.4, 1.8)	126.33, CH	6	7.71, m	128.67, CH	6
9	8.07, dd (7.7, 1.5)	130.21, CH	7	8.39, d (9.6)	125.32, CH	7/8
9a		143.77, qC	6, 8 > 9		139.30, qC	6, 7/8
1'		139.93, qC	3', 5'		128.81, qC ^e	3', 5' > 7'
2'	7.43, d (8.3, 1.3)	129.82, CH	4', 6'	7.18, d (8.4)	130.60, CH	7', 2'/6'
3'	7.24, m	129.24, CH	5'	6.74, d (8.6)	116.60, CH	5', 2'/6'
4'	7.15, m	127.16, CH	2', 6'	4.86, s	157.62, CO	2'/6', 3'/5'
5'	7.24, m	129.24, CH	3'	6.74, d (8.6)	116.60, CH	3'/5' > 2'/6'
6'	7.43, d (8.3, 1.3)	129.82, CH	2', 4'	7.18, d (8.4)	130.60, CH	7', 2'/6'
7'	4.57, s	40.95, CH ₂	2', 6'	4.60, s	38.64, CH ₂	2'/6'

^a In acetone-*d*₆, ¹H/¹³C 600/150 MHz. ^b In methanol-*d*₄, ¹H/¹³C 300/75 MHz. ^c ¹³C data are given with two digits in order to discriminate between narrowly separated signals. ^d Not observed due to H/D exchange of 7'-H₂. ^e Interchangeable.

(C-4') at $\delta_{\text{C}} = 157.6$ ppm provided HMBC correlations with the overlapping signals of H-5'/H-3' and H-2'/H-6' and allowed the assignment of the phenol unit. The signal of the bridging methylene group C-7' was detected as a singlet at $\delta_{\text{H}} = 4.60$ ppm. An HMBC correlation of C-7' with H-2' and H-6' and the only HMBC correlation of C-2 with H-7' in **4** indicated the direct connection to the marinoquinoline core structure. Similar to **3** a slow H/D exchange of the methylene group in **4** was observed.

The [M + H]⁺ ion of marinoquinoline E (**5**) appeared at *m/z* 284.1182 in the HRESIMS analysis, indicating the molecular formula C₁₉H₁₃N₃. Again the NMR spectra showed the presence of the pyrroloquinoline core structure (Table 3). However, the otherwise higher order multiplet of H-7 and H-8 was separated in **5**, due to the enlarged conjugated system. The latter was assigned from the COSY correlations from H-4' to H-7' and the HMBC correlations observed between C-7'a and H-2', -4', and -6' and between C-3'a and H-2', -5', and -7'.

The molecular formula of marinoquinoline F (**6**) C₂₀H₁₃N₃O was derived from the HRESIMS analysis of the [M + H]⁺ ion at *m/z* 312.1138. Thus **6** contains an additional CO group compared to **5**. In the ¹H NMR spectrum all signals were complex due to the second-order multiplets of H-7 and H-8 and H-5' and H-6', respectively. Nevertheless, the pyrroloquinoline core structure in **6** was easily recognized in the NMR data (Table 3) as well as an indole moiety from correlations similar to those described for **5**. The additional carbonyl carbon C-8' was detected at $\delta_{\text{C}} = 189.0$, a shift characteristic for a ketone. However, reliable HMBC correlations to the ketone carbon were not detected, and the only possible position was as a bridge between both aromatic systems. Advantageously, in addition to the NOE between H-5 and H-6, which was also observed previously in marinoquinoline A (**1**), a weaker correlation between H-9 and H-2' was detected in the ROESY spectrum of marinoquinoline F (**6**). Consistent with

these NOEs, the distances of H-5 to H-6 and H-9 to H-2' were 2.50 and 3.33 Å, respectively, in an MM2-generated model of **6**. Noticeably, the singlet of the 2'-H proton was shifted about 1.4 ppm downfield to $\delta = 9.7$ ppm. This deshielding can also be explained from the nearly planar model, which brings the indole methine H-2' into the region affected by the carbonyl anisotropy.⁷

Pityriacitrin (**8**), a UV-absorbing metabolite of the yeast *Malassezia furfur*, is a closely related isomer of **6** featuring a core structure derived from harman (**7**).⁸ The indole moiety attached to the carbonyl carbon was present in both. Consequently, comparison of the ¹H NMR data of **6** and **8** in CD₃CN showed a high similarity for the indole signals.

Screening of marinoquinolines A–F (**1**–**6**) for antibiotic activity against a broad panel of bacteria and fungi showed weak activity with a minimum inhibition concentration (MIC) of 33.5 μg/mL against some of the strains tested (Table S27). The indole variant **5** showed the broadest activity, inhibiting Gram-positive bacteria (*Nocardia flava* and *Micrococcus luteus*) and three fungi (*Schizosaccharomyces pombe*, *Mucor hiemalis*, and *Rhodotorula glutinis*), followed by the phenyl derivative **3**, with antifungal activity only (*S. pombe* and *R. glutinis*) (MIC for all 33.5 μg/mL). Both marinoquinolines A (**1**) and F (**6**) were active against Gram-negative *Escherichia coli* and *S. pombe*, at 33.5 μg/mL, respectively, while the phenyl variant **4** and isopropyl variant **2** were not active at 33.5 μg/mL in any test. When the marinoquinolines **1**–**6** were evaluated for cytotoxicity against three growing cancer cell lines and a primary cell line (Table 4), they showed only moderate cytotoxicity compared to vinblastin and epothilon. The keto-indole variant **6** was the most toxic (0.3 μg/mL, KB-3-1) followed by the phenyl derivatives **3** (0.55 μg/mL, HUVEC) and **4** (1.1 μg/mL, L929), while the isopropyl variant **2** showed the least cytotoxicity.⁹

Table 3. NMR Spectroscopic Data of Marinoquinolines E (5) and F (6) in Acetone- d_6 ($^1\text{H}/^{13}\text{C}$ 600/150 MHz)

C/H	5				6		
	δ_{H} , m (J in Hz)	$\delta_{\text{C}}^{\text{c}}$	$^1J_{\text{C,H}}$ [Hz]	HMBC ^d	δ_{H} , m (J in Hz)	$\delta_{\text{C}}^{\text{c}}$	HMBC ^d (1J [Hz])
2		144.50, qC		4		143.23, qC	
2a		128.04, qC		4 >5		131.43, qC	4, 5
NH	10.79, br s ^a				11.59, br s		
4	7.61, d (2.9)	127.50, CH	184	5	7.79, d (2.9)	129.24, CH	5
5	7.20, d (2.9)	102.24, CH	174	4	7.25, d (2.9)	101.34, CH	4 (174 Hz)
5a		129.67, qC		6, 4, 5		128.95, qC	4, 5
5b		123.72, qC ^e		9, 7 >6 ^b		125.85, qC	7, 9
6	8.27, dd (8.1, 1.5)	123.71, CH	158	8 ^b	8.39, dd (7.5, 2.0)	124.08, CH	7, 8
7	7.51, ddd (8.1, 6.9, 1.1)	125.62, CH	160	9	7.70, td (6.6, 1.8)	128.38, CH	9
8	7.57, ddd (8.2, 6.9, 1.5)	126.48, CH	159	6	7.68, td (7.5, 1.8)	127.02, CH	6
9	8.17, dd (8.1, 1.1)	129.94, CH	159	7	8.30, dd (7.7, 1.5)	131.58, CH	7
9a		143.94, qC		8, 6 > 9		142.40, qC	6, 8
NH	10.95, br s ^a				11.24, br s		
2'	8.25, br s	126.91, CH			9.70, s	139.19, CH	
3'		115.12, C		2' >4'		115.94, qC	2'
3'a		127.83, qC		7', 5' >2'		128.71, qC	2', 5', 7'
4'	8.74, d (7.3 br.)	123.64, CH	164	6' >5'	8.65, dd (6.6, 2.5)	123.31, CH	5', 6'
5'	7.21, td (7.2, 1.0 br)	121.17, CH	159	7' >4'	7.29, td (7.3, 1.8)	124.05, CH	4', 7'
6'	7.25, ddd (7.8, 7.1, 0.9)	123.43, CH		4'	7.31, td (7.5, 1.4)	123.16, CH	7'
7'	7.53, d (7.8 br)	112.33, CH	184	5'	7.60, m	112.89, CH	5'
7'a		137.93, qC		4', 6', 2'		137.14, qC	2', 4', 6'
8'						189.01, qC	

^a Interchangeable. ^b C-5b overlapping with C-6 was assigned from strong HMBC-correlations with H-9 and H-7 at this position, which should not be present if only carbon-6 was located there. Further there is a weak correlation with H-6 at this position, which is not possible for C-6. ^c ^{13}C data are given with two digits in order to discriminate between narrowly separated signals. ^d HMQC and HMBC spectra with enhanced ^{13}C resolution. ^e Quaternary carbons were observed in an APT ^{13}C NMR spectrum.

Table 4. Cytotoxicity (IC_{50} $\mu\text{g}/\text{mL}$) of Marinoquinolines A–F (1–6) against Growing Cell Lines

compound	L929	MCF-7	KB-3-1	HUVEC
1	5.5	3.5	2.2	1.5
2	8.0	6.5	5	3.6
3	5.4	2.6	2.0	0.55
4	1.1	3.2	3.2	2.5
5	5.5	1.9	4.5	5.8
6	4.1	1.6	0.3	2.8
epothilon	1.4×10^{-3}		1.2×10^{-3}	
vinblastin	18×10^{-3}		8.6×10^{-3}	

The increasing resistance against antimalarial drugs necessitates the screening of diverse sources for new lead compounds against *Plasmodium falciparum* and other tropical parasites. For example nostocarboline (9) from the cyanobacterium *Nostoc* 78-12A,¹⁰ which can be seen as a halogenated isomer of marinoquinoline A (1), showed selective activity against *P. falciparum* K1 with an IC_{50} of $0.194 \mu\text{M}$.¹¹ The IC_{50} value of 3H-pyrrolo[2,3-*c*]quinoline, the core alkaloid part of the marinoquinolines, was determined as $6.4 \mu\text{M}$.¹² In a screening test against tropical parasites (Table 5) marinoquinolines B (2) and F (6) were identified as the most active structural variants, with IC_{50} values of 1.8 and $1.7 \mu\text{M}$, respectively. However, the IC_{50} values against the cell line

L6 indicated a considerably higher cytotoxicity compared to 3H-pyrrolo[2,3-*c*]quinoline (IC_{50} $173.2 \mu\text{M}$).¹²

EXPERIMENTAL SECTION

General Experimental Procedures. The melting point was measured on a Büchi-510 melting point apparatus. UV data were recorded on a Shimadzu UV/vis-2450 spectrophotometer using methanol (UVASOL, Merck) as solvent. IR data were recorded on a Bruker Tensor 27 IR spectrophotometer. ^1H NMR and ^{13}C NMR spectra were recorded on a Bruker Avance DMX 600 or DPX 300 NMR spectrometer, locked to the deuterium signal of the solvent. Data acquisition, processing, and spectral analysis were performed with standard Bruker software and ACD/NMRWorkbook. Chemical shifts are given in ppm and coupling constants in Hz. HRESIMS data were recorded on a Maxis spectrometer (Bruker Daltonics), and molecular formulas were identified by including the isotopic pattern in the calculation (SmartFormula algorithm). Analytical RP HPLC was carried out on an Agilent 1100 HPLC system equipped with a UV diode-array detector and an evaporative light-scattering (PLE-ELS 1000) detector. HPLC conditions: column 125×2 mm, Nucleodur C-18, 5 μm (Macherey-Nagel), solvent A: 5% acetonitrile in water, 5 mmol of NH_4Ac , 0.04 mL of CH_3COOH ; solvent B: 95% acetonitrile, 5 mmol of NH_4Ac , 0.04 mL of CH_3COOH ; gradient system: 10% B increasing to 100% in 30 min, 100% B for 10 min, to 10% B post-run for 10 min; 40 °C; flow rate 0.3 mL/min. A Sephadex LH-20 column (1000×50 mm) was connected to a fraction collector (Pharmacia LKB Superfac), a plotter, and a UV detector set at 227 nm (Pharmacia).

Table 5. Antiprotozoal Activity and Cytotoxicity of Marinoquinolines A–F (1–6) (IC₅₀ [μ M])

compound	<i>Trypanosoma brucei rhodesiense</i>	<i>Trypanosoma cruzi</i>	<i>Leishmania donovani</i>	<i>P. falciparum</i> K1	cytotoxicity L6
1	54.4	29.5	>548.8	9.8	30.6
2	45.9	53.1	86.5	1.8	58.7
3	42.2	28.3	58.8	5.5	39.1
4	61.2	27.0	119.9	15.0	66.4
5	51.5	23.6	63.9	7.6	35.6
6	39.0	21.8	16.1	1.7	12.5
reference drugs ^a	0.012	1.95	0.386	0.141	0.021

^a See Table 6.

Table 6. Reference Drugs

parasite	strain/cells	stage	reference drug
<i>T. b. rhodesiense</i>	STIB 900	trypomastigotes	melarsoprol
<i>T. cruzi</i>	Tulahuen C4	amastigotes	benznidazole
<i>L. donovani</i>	MHOM-ET-67/L82	axenic amastigotes	miltefosine
<i>P. falciparum</i>	K1	IEF	chloroquine
cytotoxicity	L6 cells		podophyllotoxin

Strain O. kribbensis. The type strain PWU 25 was isolated in December 1995 from a soil sample with plant residues collected at Kukrail Reserve Forest and Crocodile Research Center, Uttar Pradesh, India, in March 1995. It was identified as *O. kribbensis* by 16S rDNA analysis.

Fermentation. For production of compounds to be isolated, a 70 L large-scale fermentation of *O. kribbensis* PWU 25 was performed in a medium containing 0.4% skimmed milk, 0.4% defatted soy flour, 0.2% yeast extract, 1.0% starch, 0.1% MgSO₄·7H₂O, 8 mg/L Fe-EDTA, 0.5% glycerin, and 2% of Amberlite XAD-16 resin, in a 100 L bioreactor (B. Braun) that was inoculated with 3 L of shaking cultures grown for 3 days in the same medium with 50 mM HEPES. The bioreactor was kept at 30 °C, aerated at 0.05 vvm per minute, pH regulated at 7.4, and agitated with a flat-blade turbine stirrer at 100 rpm.

Extraction and isolation. The fermentation was terminated after three days, and the adsorber resin and the cell mass (4320 g) were collected by sieving and centrifugation, respectively. The adsorbent resin was extracted in a glass column (70 × 8 cm) with methanol (4 L) and a final elution with acetone (4 L) at a flow rate of 2 L per hour. The solvents were evaporated to yield 10.41 g of methanol extract and 7.08 g of acetone extract. Lipophilic compounds in the methanol extract were removed by partitioning with heptane (9.25 g residue). The compounds were further enriched by acid–base partitioning. First, they were partitioned under acidic conditions between water containing 2% formic acid (pH 2) and ethyl acetate. The latter contained acidic and neutral compounds (2.5 g residue). After shifting the pH of the water layer to pH 11 by addition of ammonia, extraction with ethyl acetate and subsequent evaporation yielded 692 mg of basic extract. This was prepurified by column chromatography with Sephadex LH-20 with methanol as solvent. The fraction containing the major compound **1** was evaporated and subjected to crystallization and recrystallization in acetone–petrol ether (1:1), yielding 62.5 mg of colorless, needle-shaped single crystals, whose X-ray crystallography data were identical to those described for 4-methyl-3H-pyrrolo[2,3-*c*]quinoline.² The byproduct were further purified by preparative RP HPLC [column 250 × 21 mm Nucleodur C₁₈ (Macherey-Nagel), solvents; A: 0.5% HCOOH in 80% H₂O and solvent B: 0.5% HCOOH in 50% CH₃OH; gradient 7% B, 60 min to 83% B, 30 min 100% CH₃OH; flow rate 20 mL/min, UV detection at 240 nm], affording **2** (16.5 mg), **3** (7.5 mg), **4** (23 mg), **5** (15.3 mg), and **6** (3 mg). All pure fractions of **1** were pooled to give a final yield of 232 mg.

Marinoquinoline A (1): colorless needles; mp 236–237 °C; UV (MeOH) λ_{\max} (log ϵ) 239 (4.561), 300 (4.034), 312 (3.960), 326 (3.792) nm, IR (KBr) ν_{\max} 3442, 2924, 2854, 1631, 1587, 1441, 1366, 1125, 1026 cm⁻¹; for NMR data see Table 1; HRESIMS m/z 183.0919 [M + H]⁺ (calcd for C₁₂H₁₀N₂, 183.0922).

Marinoquinoline B (2): colorless, amorphous solid; UV (MeOH) λ_{\max} (log ϵ) 226 (4.651), 240 (4.678), 301 (4.093), 314 (4.028), 327 (3.867) nm; for NMR data see Table 1; HRESIMS m/z 225.1382 [M + H]⁺ (calcd for C₁₅H₁₆N₂, 225.1386).

Marinoquinoline C (3): colorless, amorphous solid; UV (MeOH) λ_{\max} (log ϵ) 228 (4.755), 239 (4.751), 302 (4.154), 314 (4.101), 329 (3.959) nm; for NMR data see Table 2; HRESIMS m/z 259.1236 [M + H]⁺ (calcd for C₁₈H₁₄N₂, 259.1230).

Marinoquinoline D (4): colorless, amorphous solid; UV (MeOH) λ_{\max} (log ϵ) 227 (4.823), 240 (4.816), 302 (4.233), 315 (4.186), 329 (4.032) nm; for NMR data see Table 2; HRESIMS m/z 275.1181 [M + H]⁺ (calcd for C₁₈H₁₄N₂O, 275.1179).

Marinoquinoline E (5): yellow, amorphous solid; UV (MeOH) λ_{\max} (log ϵ) 225 (4.564), 242 (4.451), 306 (4.018), 315 (4.009), 339 (4.009) nm; for NMR data see Table 3; HRESIMS m/z 284.1182 [M + H]⁺ (calcd for C₁₉H₁₃N₃, 284.1182).

Marinoquinoline F (6): yellow oil; UV (MeOH) λ_{\max} (log ϵ) 210 (4.638), 222 (4.602 sh), 271 (4.050 sh), 328 (3.866), 361 (3.739) nm; for NMR data in methanol-*d*₄ see Table 3; ¹H NMR (600 MHz, CD₃CN) δ ppm 11.06 (1H, br s, H-3), 7.71 (1H, m, H-4), 7.18 (1H, t, J = 2.2 Hz, H-5), 8.34 (1H, m, H-6), 7.68 (1H, m, H-7), 7.66 (1H, t, J = 2.8 Hz, H-8), 8.32 (1H, m, H-9), 10.13 (1H, br s, H-1') 9.56 (1H, d, J = 2.9 Hz, H-2'), 8.58 (1H, dd, J = 6.6, 1.8 Hz, H-4'), 7.32 (1H, td, J = 7.2, 1.5 Hz, H-5'), 7.34 (1H, td, J = 7.3, 1.5 Hz, H-6'), 7.59 (1H, dd, J = 6.4, 2.0 Hz, H-7'); HRESIMS m/z 312.1138 [M + H]⁺ (calcd for C₂₀H₁₃N₃O, 312.1131).

Minimum Inhibition Concentration Assays. The MIC of marinoquinoline A–F was tested against the Gram-positive bacteria *Staphylococcus aureus*, *N. flava*, and *M. luteus* and the Gram-negative bacteria *E. coli* and *Chromobacterium violaceum*. In addition to the fungi *M. hiemalis*, the yeasts *Candida albicans*, *R. glutinis*, and *Pichia anomala* and the fission yeast *S. pombe* were also tested. MIC tests were conducted in 96-well microtiter well plates in EBS medium¹³ for bacteria and MYC medium (1.0% phytone peptone, 1.0% glucose, 50 mM HEPES [11.9 g/L] pH 7.0) for yeasts and fungi, respectively. First, 10 μ L aliquots of each of the marinoquinolines A–F at 1 mg/mL in MeOH and 2 μ L for the reference drugs (broad spectrum antibiotic oxytetracycline hydrochloride (Sigma) at 1 mg/mL in Millipore water and antifungal nystatin (Sigma) at 1 mg/mL in MeOH) were pipetted on the first row (A) of the plate, and a few minutes allowed for the solvents to evaporate. Negative control wells were left blank. Using a multi-channel pipet, 150 μ L of a mixture of the test pathogen and the culture medium in the ratio of 1:100, respectively, was aliquoted in all the rows. To the first row, an additional 150 μ L of the pathogen-medium mixture was added and mixed by repeated pipetting, before transferring the

same amount to the second row. A 1:1 serial dilution was done in the subsequent rows, and 150 μL discarded after the last row (H). Plates were incubated on a microplate-vibrating shaker (Heidolph Titramax 1000) at 600 rpm at 30 °C for 24–48 h. The lowest concentration of the drug preventing visible growth of the pathogen was taken as the MIC. The concentrations tested ranged from 33.5 to 0.052 $\mu\text{g}/\text{mL}$.

Cytotoxicity Assay. *In vitro* cytotoxicity (IC_{50}) was determined against a panel of mammalian cell lines including the breast cancer cell line MCF-7, the cervix carcinoma cell line KB-3-1, the established mouse fibroblast cell line L929, and the nontransformed human umbilical vein endothelial cell line (HUVEC). KB-3-1 and L929 were cultured in DMEM (Lonza), HUVEC was cultured in EBM-2 (Lonza), and MCF-7 was cultured in RPMI (Lonza) media, all supplemented with 10% of fetal bovine serum (Gibco) under 10% CO_2 at 37 °C. The cytotoxicity assay was performed according to the MTT (3-(4,5-dimethylthiazol-2-yl)-2,5-diphenyltetrazolium bromide) method in 96-well microplates (Mosmann, 1983). Briefly, 60 μL aliquots of serial dilutions from an initial stock of 1 mg/mL in MeOH of the test compounds were added to 120 μL aliquots of a cell suspension (50 000/mL) in 96-well microplates. After 5 days incubation, a MTT assay was performed, and the absorbance measured at 590 nm using an ELISA plate reader (Victor). The concentration at which the growth of cells was inhibited to 50% of the control (IC_{50}) was obtained from the dose–response curves. Negative control was methanol (Table 4).

Antiprotozoal Activity and Cytotoxicity Assay (Table 5). Determined as described in the literature.^{11,12}

■ ASSOCIATED CONTENT

S Supporting Information. Copies of 1D and 2D NMR spectra of marinoquinolines A–F (1–6), photos of vegetative cells and growth on agar of *Ohtaekwangia kribbensis*, strain PWU 25, and a table of antibacterial and antifungal activities (MIC). This material is available free of charge via the Internet at <http://pubs.acs.org>.

■ AUTHOR INFORMATION

Corresponding Author

*Tel: +49-681-30270201. Fax: +49-681-30270202. E-mail: rom@mx.uni-saarland.de.

■ ACKNOWLEDGMENT

P.W.O. is indebted to the Deutscher Akademischer Austauschdienst (DAAD) for a PhD scholarship. We thank C. Kakoschke and B. Jaschok-Kentner for NMR spectroscopic measurements, Dr. F. Sasse for cytotoxicity assays, Prof. R. Brun [Swiss Tropical and Public Health Institute (Swiss TPH)] and M. Kaiser (Swiss TPH) for screening against tropical parasites, W. Kessler for large-scale fermentation, and K. Schober, A. Teichmann, D. Telkemeyer, and W. Collisi for technical assistance.

■ REFERENCES

- (1) Srisukchayakul, P.; Suwanachart, C.; Sangnoi, Y.; Kanjana-Opas, A.; Hosoya, S.; Yokota, A.; Arunpaiojana, V. *Int. J. Syst. Evol. Microbiol.* **2007**, *57*, 2275–2279.
- (2) Kanjana-opas, A.; Panphon, S.; Fun, H.; Chantrapromma, S. *Acta Crystallogr.* **2006**, *E62*, 2728–2730.
- (3) Sangnoe, Y.; Sakulkeo, O.; Yuenyongsawad, S.; Kanjana-opas, A.; Ingkaninan, K.; Plubrukarn, A.; Suwanborirux, K. *Mar. Drugs* **2008**, *6*, 578–586.
- (4) Yoon, J. H.; Kang, S. J.; Lee, S. Y.; Lee, J. S.; Park, S. *Int. J. Syst. Evol. Microbiol.* **2010** (in press) doi: 10.1099/ijs.0.025874-0.

(5) *Dictionary of Natural Products on DVD*, Ver. 19.1, CRC Press: London, UK, 2010.

(6) In a pyridine-type ring a vicinal coupling of about 5.5 Hz would be expected. In a simple pyridine ring the direct H,C coupling of methine 5 would be expected near 163 Hz compared to 168 Hz for a corresponding pyrrole.

(7) Abraham, R. J.; Mobli, M.; Smith, R. J. *Magn. Reson. Chem.* **2003**, *41*, 26–36.

(8) Mayser, P.; Schäfer, U.; Krämer, H. J.; Irlinger, B.; Steglich, W. *Dermatol. Res.* **2002**, *294*, 131–134.

(9) Mosmann, T. J. *Immunol. Methods* **1983**, *65*, 56–63.

(10) Becher, P. G.; Beuchat, J.; Gademann, K.; Jüttner, F. *J. Nat. Prod.* **2005**, *68*, 1793–1795.

(11) Bonazzi, S.; Barbaras, D.; Patiny, L.; Scopelliti, R.; Schneider, P.; Cole, S. T.; Kaiser, M.; Brun, R.; Gademann, K. *Biorg. Med. Chem.* **2010**, *18*, 1464–1476.

(12) Van Baelen, G.; Hostyn, S.; Dhoooghe, L.; Tapolcsanyi, P.; Matyus, P.; Lemiere, G.; Dommissie, R.; Kaiser, M.; Brun, R.; Cos, P.; Maes, L.; Hajos, G.; Riedl, Z.; Nagy, I.; Maes, B. U. W.; Pieters, L. *Biorg. Med. Chem.* **2009**, *17*, 7209–7217.

(13) Shimkets, L. J.; Dworkin, M.; Reichenbach, H. . In *The Prokaryotes: A Handbook on the Biology of Bacteria*; Dworkin, M., Falkow, S., Rosenberg, E., Schleifer, K. H., Stackebrandt, E., Eds.; Springer: New York, 2006; Vol. 7, pp 31–115.